

# Effect of silicon on microstructure and stress rupture properties at 1100°C of yttrium modified Ni-Al-Mo-B alloy IC6

C. B. XIAO, Y. F. HAN

Beijing Institute of Aeronautical Materials (BIAM), P.O. Box 81-1,  
Beijing 100095, People's Republic of China  
E-mail: CBXiao@263.net

The effect of adding 0.10–0.30 wt%Si on microstructure of the yttrium modified alloy IC6 was examined by scanning electron microscope (SEM), energy dispersive spectrum(EDS) technique of electron probe micro-analyzer (EPMA) and transmission electron microscope (TEM). The results show that two bulk shape phases,  $\text{Mo}_{1.24}\text{Ni}_{0.76}$  and  $\text{Mo}_6(\text{Ni}_{0.75}\text{Si}_{0.25})_7$  are formed in the interdendritic area in the alloy with addition of 0.10–0.20 wt%Si and 0.12 wt%Y, and that a needle like phase named Y-NiMo precipitates in the interdendritic area in the alloy with addition of 0.30 wt% silicon and 0.12 wt% yttrium besides the formation of the bulk shape phases mentioned above. The stress rupture properties under 1100°C/80 MPa were improved by adding 0.12 wt%Y but decreased by adding 0.10–1.30 wt%Si and 0.12 wt%Y. © 2001 Kluwer Academic Publishers

## 1. Introduction

A directionally solidified alloy IC6 with the chemical composition of Ni-(7.5–8.5)Al-(13.0–15.0)Mo-(0.02–0.1)B wt% has been recently developed in BIAM as a high-temperature structural material used for advanced jet-engine blades and vanes operating in the temperature range of 1050–1150 °C [1]. The alloy not only has high yield strength and fairly good ductility from room temperature to 1100 °C, but also has high creep resistance in the temperature range of 760–1100 °C. Alloy IC6 has low density (7.9 g/cm<sup>3</sup>), low cost, high incipient melting temperature (1300 °C). Its high temperature oxidation resistance is substantially improved by adding proper amount of yttrium [2, 3], and silicon can further improve the high temperature oxidation resistance and hot corrosion resistance of the yttrium modified alloy IC6 [4]. The purpose of the present work is to investigate the effect of silicon on microstructure and high temperature stress rupture properties of yttrium modified alloy IC6.

Silicon may be used as refining additions during melting. However, with some exceptions, its presence in the final alloys is considered harmful to the mechanical properties and the therefore upper limit is usually controlled at a low level, and its harmful effect is usually caused by the phase change due to the presence of silicon. Rizzo and Buzzanell [5] found that silicon promotes the formation of  $\text{M}_6\text{C}$  and stabilizes the Laves phase and hence decreases the room temperature ductility of alloy Unitemp 718. Mason and Rawlings [6] reported that the presence of Si in (wt%) 50Ni-32Mo-2Si-15Cr increases the proportion of primary phase, stabilizes the hexagonal form of Laves phase and pro-

duces an ill defined eutectic. Silicon (0.4 wt%) increases the formation of  $\gamma$ /Laves constituent and promotes formation of  $\gamma$ / $\text{M}_6\text{C}$  constituent at low levels (<0.01 wt%) of C, while promotes the  $\gamma$ / $\text{MC}$  and  $\gamma$ /Laves constituents at higher levels (0.035 wt%) of C in Alloy 625 [7]. Durber *et al.* [8] found that there were little microporosity and increased amount of a phase rich in Ni and Hf which induces a slight decrease in stress rupture properties in Si doped nickel base superalloy MAR-M002. Guo and Zhou [9] reported that Si promotes the segregation of niobium and formation of Laves phase, raises the  $\gamma$ /Laves eutectic reaction temperature and decreases the tensile strength and ductility of cast alloy 718. In IN738 superalloy [10], Si segregates mainly in interdendritic regions and promotes the segregation of other elements, Si affects the morphology of the liquid-solid interface of the alloy during solidification and gives the alloy a tendency to form well-developed dendrites, Si also enlarges the solidus-liquidus temperature interval. Tsutsumi and Takahashi [11] found that the solidification cracking susceptibility of (wt%) 70Ni-14Cr-4Mo-2Nb Inconel-type weld metal increases with increasing Si content and that the cracks are associated with the low melting point of Nb and Si precipitates formed as a result of the segregation of Si and Nb.

## 2. Experimental procedure

The master alloy was first prepared by a vacuum induction furnace, and then the columnar grain specimens with addition of different amount of silicon and yttrium were produced by rapid solidification technique in a

commercial DS vacuum induction furnace. The as-cast specimens were homogenized at 1260 °C for 10 h with oil-quenching.

The size of the specimens for stress rupture tests is 5 mm in diameter and 25 mm in gauge length. The stress rupture tests were carried out in air by using constant load creep machines at 1100 °C, with the testing temperatures controlled within  $\pm 5^\circ\text{C}$ .

The specimens after homogenization for microstructural analysis were polished and etched in the solution of 25 vol% nitric acid, 50 vol% hydrofluoric acid and 25 vol% glycerin, and then examined in a JSM-35 scanning electron microscope (SEM) and a JXA 8600 electron probe micro-analyzer (EPMA). The thin foils for TEM study were done by twin-jet electrolytic polishing from a starting thickness of 30–40  $\mu\text{m}$  using 17 vol.% perchloric acid and 83 vol.% alcohol solution under conditions of about 90 V at  $-20^\circ\text{C}$  or below and then examined in a JEM 2010 transmission electron microscope under 200 kV. The micro-hardness of precipitates due to the addition of silicon was analyzed in MVK-E at room temperature.

### 3. Results and discussion

#### 3.1. Effect of silicon on microstructure of the yttrium modified alloy IC6

The microstructure of alloy IC6 after homogenization at 1260 °C for 10 h and oil quenching was examined by SEM. The results showed that the microstructure of alloy IC6 can be divided into interdendritic and dendritic areas, A and B respectively, as shown in Fig. 1. The volume percent of  $\gamma$  phase is about 20–25% and that of  $\gamma'$  phase is about 75–80%. The dimension of  $\gamma'$  precipitates is 0.1–0.3  $\mu\text{m}$  in interdendritic area and 1–3  $\mu\text{m}$  in dendritic area. Boride usually appears in the interdendritic area when boron content exceeds 0.16 at% [12]. The results of SEM also showed that the microstructure of alloy IC6 with addition of 0.12 wt% yttrium has no obvious difference compared with that of alloy without yttrium [2, 13]. Some bulk shape phases (white color) are formed in the interdendritic area of the alloy with addition of 0.10–0.20 wt% Si and 0.12 wt% Y, as shown

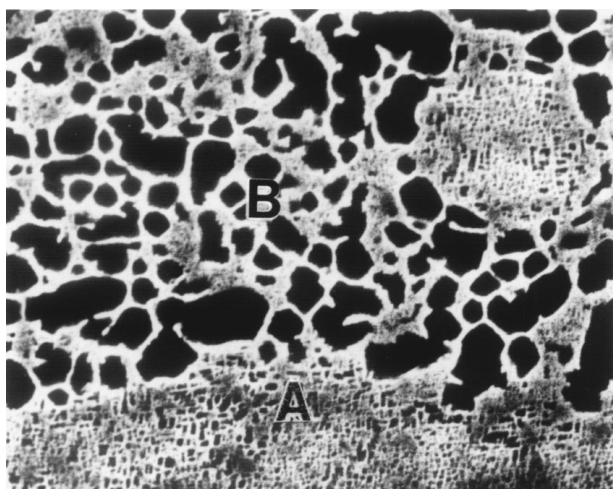


Figure 1 SEM image of homogenized specimen of alloy IC6.

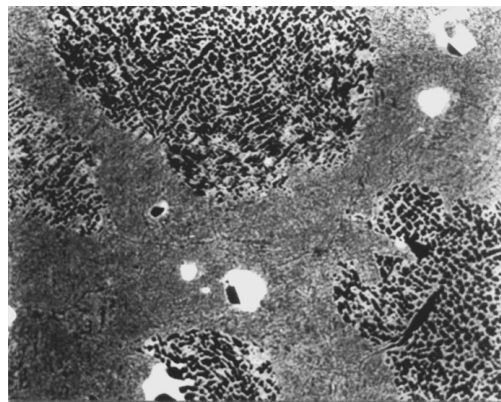


Figure 2 Back scattered electron image (BSEI) of alloy with 0.10–0.20 wt% Si and 0.12 wt% Y.

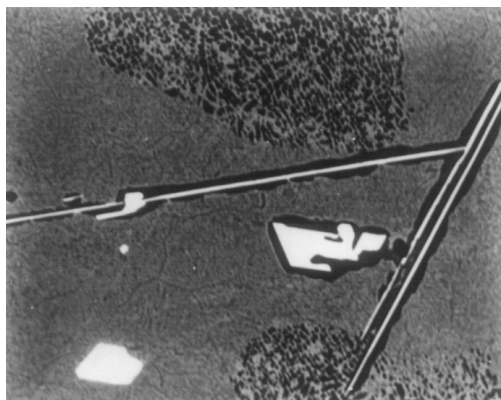


Figure 3 Back scattered electron image (BSEI) of alloy with 0.30 wt% Si and 0.12 wt% Y.

in Fig. 2. The volume percent of the bulk shape phases increases with the increasing addition amount of silicon. The EDS results show that there are two kinds of bulk shape phases in Fig. 2, one containing Si and the other one containing no Si. The conventional TEM analysis results show that the bulk shape phase containing Si is  $\text{Mo}_6(\text{Ni}_{0.75}\text{Si}_{0.25})_7$  and the one containing no Si is  $\text{Mo}_{1.24}\text{Ni}_{0.76}$  [14].

Besides the formation of the bulk shape phases mentioned above, a needle like phase enveloped by large size  $\gamma'$  phase precipitates in the interdendritic area in the alloy with addition of 0.3 wt% Si and 0.12 wt% Y, as shown in Fig. 3. The chemical composition of the needle like phase is analyzed to be 46.9Ni–49.7Mo–3.4Al(at%) by EDS of EPMA. The atomic percentage ratio between Ni and Mo is about 1. Conventional TEM analysis results indicated that the needle like phase has the same crystal structure as that of Y–NiMo phase precipitated during the aging at 900–1150 °C in alloy IC6 [15].

#### 3.2. Stress rupture properties

The stress rupture lives under 1100 °C/80 MPa of alloy IC6 and alloys with different amount of silicon and yttrium are shown in Fig. 4. The results in Fig. 4 show that the stress rupture life of alloy with 0.12 wt% Y is longer than that of alloy IC6 without yttrium, the improvement in stress rupture life for alloys with addition of yttrium

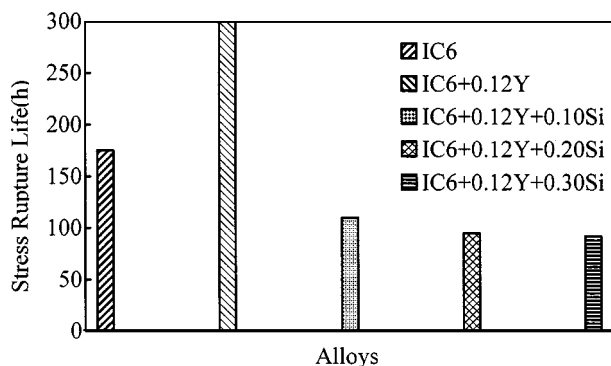


Figure 4 Stress rupture lives under 1100°C/80 MPa of alloys with different amount of yttrium and silicon.

may be attributed to the following three roles played by yttrium: (a) Substantially improving the oxidation resistance of alloy IC6 [3, 16]. The stress rupture tests were carried out with constant load in air at 1100°C. The oxide scale spalled easily at 1100°C for alloy without yttrium, which induced the rapid increment of real stress. While for the alloy with addition of yttrium, the adherence of the oxide scale to the substrate is substantially improved, which makes the increasing speed of real stress slow down and the stress rupture life longer; (b) Desulfurization. Yttrium can easily react with sulfur to form sulfides of high incipient melting temperature during melting. The usual form of sulfide is  $Y_2S_3$ . The density of  $Y_2S_3$  is 3.87 g/cm<sup>3</sup>, which is much lower than that of alloy IC6.  $Y_2S_3$  is floatable in the melt and can adhere to the wall of the crucible during melting. Hence the content of sulfur remained in the alloy is decreased, which decreases the harmful effects of sulfur on materials strength; (c) Promoting the formation of a fine dendrite. Yttrium usually segregates to the interface between solid and liquid during solidification to inhibit the growth of crystal and keep a fine dendrite, which increases the strength of the alloy.

The results in Fig. 4 also show that the stress rupture properties under 1100°C/80 MPa of alloys with 0.10–0.30 wt%Si and 0.12 wt%Y decreases steadily with the increasing amount of silicon, the decrement in stress rupture property is caused by  $Mo_6(Ni_{0.75}Si_{0.25})_7$ ,  $Mo_{1.24}Ni_{0.76}$  and needle like Y-NiMo phases precipitated in the interdendritic area due to the presence of silicon (see Figs 2 and 3). The micro-hardness of these phases is much higher than  $\gamma$  and  $\gamma'$  phases, as shown in Table I. It is difficult for dislocations to slip through these phases during deformation. These phases can only be deformed through twinning, as shown in Fig. 5. The bulk shape phase illustrated in Fig. 5 is  $Mo_6(Ni_{0.75}Si_{0.25})_7$  whose micro-hardness is the lowest one among the three phases. The micro-cracks are easily formed due to the stress concentration induced by the pile up of dislocations at the interface between

TABLE I Micro-hardness of different phases

Phase	$\gamma'$	$Mo_{1.24}Ni_{0.76}$	$Mo_6(Ni_{0.75}Si_{0.25})_7$	Y-NiMo
Micro-hardness (kg f/mm <sup>2</sup> )	348	1296	653	1288

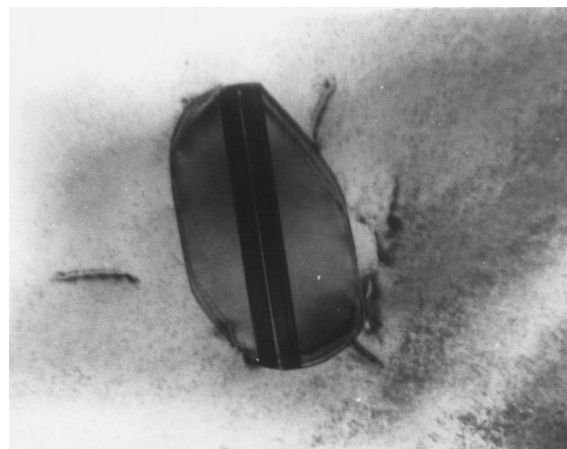


Figure 5 Bright field image of TEM showing deformation of  $Mo_6(Ni_{0.75}Si_{0.25})_7$  by twinning.

these hard phases, especially the needle like Y-NiMo phase and matrix, and hence decrease the stress rupture properties.

#### 4. Conclusions

The stress rupture properties under 1100°C/80 MPa are improved by adding 0.12 wt%Y but decreased by adding 0.12 wt% yttrium and 0.10–0.30 wt% silicon. The increment in stress rupture property can be attributed to the improvement of the high temperature oxidation resistance of the alloy, desulfurization, and formation of the fine dendrite due to the presence of yttrium. The hard phases  $Mo_{1.24}Ni_{0.76}$ ,  $Mo_6(Ni_{0.75}Si_{0.25})_7$ , and Y-NiMo which can be deformed only through twinning account for the decrement in stress rupture properties of the alloys with addition of 0.12 wt%Y and 0.10–0.30 wt%Si.

#### Acknowledgements

The authors wish to acknowledge the Advanced Materials Committee of China for the financial support.

#### References

1. Y. F. HAN, Z. P. XING and M. C. CHATURVEDI, in "Structural Intermetallics," edited by M. V. Nathal, R. Darolia, C. T. Liu, P. L. Martin, D. B. Miracle, R. Wagner, M. Yamaguchi TMS, USA (1997) p. 713. The Second International Symposium on Structural Intermetallics, Seven Springs Mountain Resort, Champion, Pennsylvania, September 21–25, 1997.
2. C. B. XIAO and Y. F. HAN, *Acta Metallurgica Sinica* **11** (1998) 296. (English Letters.)
3. *Idem.*, *ibid.* **34** (1998) 1158. (in Chinese.)
4. *Idem.*, *Materials Engineering* **8** (1998) 11. (in Chinese.)
5. F. J. RIZZO and J. D. BUZZANELL, *J. Met.* **21** (1969) 24.
6. S. E. MASON and R. D. RAWLINGS, *Mater. Sci. Technol.* **5** (1989) 180.
7. M. J. CIESLAK, T. J. HEADLEY, T. KOLLIE and A. D. ROMIG JR, *Metall. Trans.* **19A** (1988) 2319.
8. G. L. R. DURBER, S. OSGERBY and P. N. QUESTED, *Met. Technol.* **11** (1984) 129.
9. J. T. GUO and L. Z. ZHOU, in *Superalloys 1996*, Champion, Pennsylvania, USA, September 22–26, 1996 (Publ. Minerals, Metals and Materials Society/AIME, 1996) p. 451.

10. H. Q. ZHU, S. R. GUO, H. R. GUAN, Y. X. ZHU, Z. Q. HU, Y. MURATA and M. MORINAGA, *Mater. High Temp.* **12** (1994) 285.
11. S. TSUTSUMI and E. TAKAHASHI, *Kobe Res. Dev.* **39** (1989) 77. (in Japanese.)
12. Y. F. HAN, Y. M. WANG and M. C. CHATURVEDI, *J. Mater. Eng. Perf.* **2** (1993) 589.
13. C. B. XIAO and Y. F. HAN, *Scripta Materialia* **41** (1999) 475.
14. *Idem.*, *Journal of Materials Research*, in revision.
15. Y. F. HAN, S. H. LI, Y. JIN and M. C. CHATURVEDI, *Mater. Sci. & Eng. A* **192/193** (1995) 899.
16. C. B. XIAO and Y. F. HAN, *Scripta Materialia* **41** (1999) 1217.

*Received 5 October 1999  
and accepted 16 February 2000*